Fusion Engineering and Design 196 (2023) 114020

Contents lists available at ScienceDirect

Fusion Engineering and Design

journal homepage: www.elsevier.com/locate/fusengdes

Admixed pellets for fast and efficient delivery of plasma enhancement gases: Investigations at AUG exploring the option for EU-DEMO

P.T. Lang [a,*], L.R. Baylor [b], Ch. Day [c], R. Dux [a], R.M. McDermott [a], T. Giegerich [c], T. Gleiter [a], A. Kallenbach [a], B. Ploeckl [a], V. Rohde [a], A. Zito [a], ASDEX Upgrade Team [1]

[a] Max Planck Institute for Plasma Physics, Boltzmannstr. 2, Garching 85748, Germany
[b] Oak Ridge National Laboratory, Oak Ridge, TN 37830, United States
[c] Karlsruhe Institute of Technology (KIT), Karlsruhe, Germany

ARTICLE INFO

Keywords:
ASDEX Upgrade
EU-DEMO
Fuelling
Pellet

ABSTRACT

Gas and pellet injection are envisaged for particle fuelling in EU-DEMO. The gas system will provide edge and divertor fuelling and any further gas species required for operation. Pellets, mm-sized bodies formed from solid hydrogen fuel, are designed for efficient and fast core fuelling. However, they can also be employed for a more efficient delivery of plasma enhancement gases, by admixing them with the fuelling pellets. To check this option for EU-DEMO, explorative investigations have been performed at ASDEX Upgrade (AUG).

The AUG system produces ice in a batch process sufficient for about 100 pellets, initially designed for operation with pure H_2 or D_2. On a trial basis, pellet formation was tested using an H_2/D_2 mixture and admixtures containing small amounts (up to 2 mol%) of N_2, Ar, Kr or Xe in the D_2 host. A homogeneous and reproducible ice composition was found for the $H_2/D_2 = 1{:}1$ case. For all the admixed gases, a depletion of the admixture in the ice with increasing atomic number is observed. Nevertheless, the fast and efficient delivery of admixed pellets was clearly demonstrated in dedicated plasma experiments at AUG. Detailed investigations showed that the Ar supplied via admixed pellets has a higher radiation efficiency and a faster radiation rise than an Ar/D_2 gas puff. Furthermore, Ar density measurements in a discharge with admixed pellet injection show reasonable agreement with findings of a fading admixed species' concentration along the ice rod and assumptions on the pellet ablation location in the plasma. Investigations performed at the Oak Ridge National Laboratory with a large batch extruder using up to 2 mol% Ne in D_2 confirmed that production of much larger ice quantities can be achieved.

These initial explorative investigations clearly reveal the great potential of admixed pellets, although they also demonstrate that further technology efforts are required before their benefits can be utilized.

1. Introduction

A combination of gas and pellet injection is envisaged to meet the particle fuelling needs of EU-DEMO, a proposed demonstrator that a fusion power plant is feasible [1]. The gas system will provide the required edge and divertor fuelling as well as any further gas species required for operation. Pellets, mm-sized bodies formed from solid hydrogen fuel, are initially designed for efficient and fast core fuelling. However, they can potentially also be employed for a more efficient delivery of plasma enhancement gases, by admixing them with the fuelling pellets. To explore this option for EU-DEMO, investigations have been performed in the recent years.

Tests performed with the ASDEX Upgrade (AUG) pellet launching system (PLS) showed that a homogeneous and reproducible ice composition can be achieved when both stable hydrogen isotopes protium (H_2) and deuterium (D_2) are mixed H_2/D_2=1:1 [2]; also, small amounts of nitrogen (N_2) can be admixed into D_2 host pellets [3]. Supplementary investigations performed at the Oak Ridge National Laboratory (ORNL) with a large batch extruder using neon (Ne) in D_2 confirmed that production of admixed ice can be achieved, here employing even much larger ice quantities [4,5]. Considerations on the physics basis of the plasma scenarios employed for the definition of the various EU-DEMO baselines [6] initiated a request to extend these tests to Xenon (Xe). Eventually, dedicated investigations have been

* Corresponding author.
E-mail address: peter.lang@ipp.mpg.de (P.T. Lang).
[1] See author list of U. Stroth et al. 2022 Nucl. Fusion 62 042006

https://doi.org/10.1016/j.fusengdes.2023.114020
Received 22 May 2023; Received in revised form 2 September 2023; Accepted 27 September 2023
Available online 29 September 2023

performed at AUG aiming to produce pellets with any stable noble gas species admixed. Hence, during the period 2019 to 2022, in addition to Xe as well argon (Ar) and krypton (Kr) admixtures have been investigated. As detailed in the following, all the findings from this proof-of-principle investigation performed so far clearly reveal the great potential of admixed pellets, although they also demonstrate that further technology efforts are required before their benefits can be fully utilized.

In this work, the experimental setup can be found in Section 2, experimental results from an analysis of the pellet residual gas in Section 3. Admixed pellet actuator applications in plasma experiments are presented in Section 4, an analysis of the Ar plasma content in Section 5. Finally, a discussion of the actual status of the admixed pellet actuator (Section 6) and an outlook for its further development (Section 7) conclude this work.

2. Experimental setup

The AUG PLS can produce ice in a batch process sufficient for about 100 pellets of potentially different size [7]. First, the supply gas is transferred into the cold extrusion cryostat where it gets condensed. Thereafter, the ice is mechanically compressed and extruded into the storage cryostat through a 10 mm long nozzle with a square shape equivalent to the pellet cross section (1.4 mm • 1.4 mm for small and 1.9 mm • 1.9 mm for large pellets). The resulting 192 mm long ice rod is stored at a temperature of about 8 K for operation with pure D_2 or admixed ice. On demand, this rod is pushed forward by a lever and a pellet is cut from the rod into the centrifuge where it is accelerated to its final speed. Subsequently, it passes through the looping shaped guiding system into the torus as shown in Fig. 1. Initially, the system was designed only for operation with pure H_2, D_2 or their mixtures.

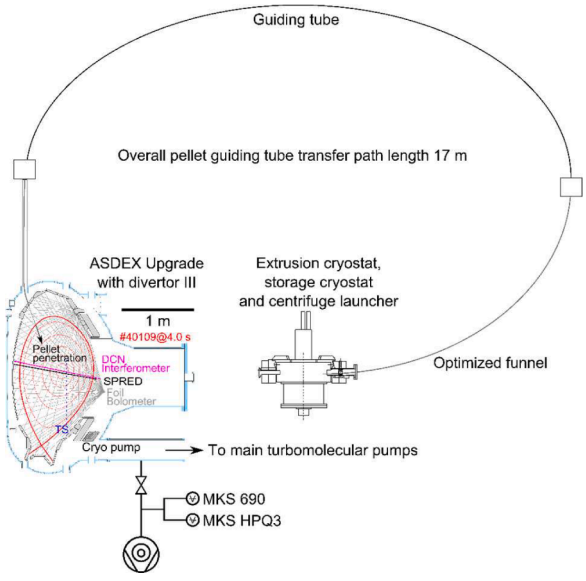

Fig. 1. Schematic setup, showing a poloidal cross section of AUG as operated during the campaigns 2019 to 2022 in the divertor III configuration. Components installed at different toroidal locations are projected into a common plane. PLS with batch extruder, storage cryostat, centrifuge launcher and looping guiding tube system. RGA system with quadrupole mass spectrometer (MKS HPQ3) and capacitive pressure gauge for calibration (MKS 690) [8] employed for analysis of the gas released from pellets injected into torus without plasma. Plasma diagnostics for experiments with pellets injected into plasma discharges: spectrometer recording extended domain SPRED, central chord of DCN laser interferometer, core Thomson scattering (TS), foil bolometer cameras and diodes. Typical pellet penetration depth indicated for the magnetic configuration of a discharge applied for the Ar [9] and Kr seeding investigations.

Therefore, mechanical stability issues of some launcher components impose restrictions when admixing heavier elements to the supply gas. Hence, rather low admixing grades in the supply gas have been chosen with their magnitude based on the respective expected specific weight of the admixed pellet. In a previous test where N_2 was admixed in situ to the D_2 host gas a level of about 1 mol% has been recognized as bearable; yet the phase change at pellet formation was associated to reduction of the N_2 component to about 0.8 mol% [3].

In this work, admixtures of Ar, Kr and Xe in the D_2 host gas were used. In order to achieve higher precision, prefabricated supply gas samples have been ordered. They were all delivered precisely characterized. Table 1 summarizes the properties of the noble gases, including their triple point temperatures (the triple point of a substance is the temperature and pressure at which its three phases gas, liquid, and solid coexist in thermodynamic equilibrium [10], data taken from [11]) and shows their recorded concentrations in the supply gas samples. Since the Ne gas sample was not delivered in time before the end of the 2022 experimental campaign, the planned investigation of the Ne admixed pellets at AUG was postponed. It will be done only after the next restart currently scheduled for mid-2024. The Ar, Kr and Xe supply gas samples were used for experiments with admixed pellets injected into the torus without and during or plasma operation.

The best characterization of the achieved concentration of the admixed species in the pellet was obtained by means of the residual gas analyzers (RGA) in pellet injection experiments without plasma operation. The RGA system is installed as shown in Fig. 1 at the AUG torus [8].

In order to analyse the impact of admixed pellets on a plasma discharge, use was made of the broad and versatile AUG diagnostics equipment in pellet injection experiments during plasma operation. All relevant information on essential plasma parameters such as confinement, density and temperature profiles were available. The plasma configuration employed for the previous Ar seeding investigation [9] was adopted for similar experiments with Kr in this work. In Fig. 1, the magnetic configuration is depicted as well as the typical pellet penetration depth, the line-of-sight (LOS) of the SPRED (for survey, poor resolution, extended domain) spectrometer, the deuterium cyanide (DCN) laser interferometer core LOS, locations of the Thomson scattering (TS) core density and temperature measurements, and the resistive foil bolometry view chords covering the full poloidal plasma cross section. Besides these diagnostics, charge exchange recombination spectroscopy (CXRS) data were analysed with the charge exchange impurity concentration analysis code (CHICA) [12] to determine local densities of certain charge states of the admixed species. In particular, Ar^{16+} densities were derived in the experiments with Ar admixed pellets, making use of recently determined CX cross-sections [13].

It is understood that the pellet plasma impact investigation bears less potential for a precise analysis of the concentration of the admixed component in the pellet composition compared to the RGA approach. However, since in this case every single pellet can be resolved and the pellets are injected within a few seconds, the relative admixed concentration evolution along the ice rod can be derived with higher spatial resolution and essentially unaffected by different storage times.

Table 1
Noble gases admixed into D_2 host gas for the investigations performed in 2019–2022. Please note that mol% is referring to the ratio of noble gas atoms to D_2 molecules; at/s flux ratios are therefore half in magnitude.

Gas	Atomic charge Z	Atomic weight (amu)	Concentration in D_2 supply gas (mol%)	Triple point temperature [K]
Ne	10	20.18	1.937± 0.039	24.6
Ar	18	39.95	2.037± 0.041	83.8
Kr	36	83.80	1.278± 0.026	115.8
Xe	54	131.29	0.205± 0.004	161.4

3. Results of the residual gas analysis

In order to measure the admixed components concentration in the pellets, their residual gas was analysed. For this residual gas analysis, pellets were injected into the evacuated but unpumped torus vessel (vessel pumps' gate valves closed, cryo-pump warm). It is assumed that pellets get smashed when impacting on the vessel tungsten (W) wall with the released gas composition reflecting the pellet composition. This sublimate is pumped through the MKS HPQ3 quadrupole mass spectrometer (QMS). The partial pressure of both, the D_2 host as well as the admixed species, can be obtained from the recorded mass spectrum after calibration of the QMS for the respective species. Therefore, a calibration run was performed for every admixed noble gas using the absolute capacitance MKS 690 type manometer. An initial pure D_2 puff was followed by an increasing admixture of puffed noble gas. The partial gas pressures were determined from the total pressure measurement and matched with the recorded intensities in the QMS spectra. Evidently for the noble gases their isotopic abundance had to be considered, which was always found to reflect well the natural distribution.

For the ice preparation, a specified amount of the admixed supply gas held at room temperature was released into the cold extrusion cryostat. Inside this extrusion batch cryostat, kept at the same operational parameters used for pure D_2, a part of the provided supply gas gets frosted and then extruded through a nozzle into the storage cryostat. In the storage cryostat, the extruded ice rod is kept until, upon request, a stepping motor driven lever pushes the ice to the cutter. At the exact cutting time, synchronized to the centrifuge revolution, the pellet is cut out of the extruded rod, dropped into the centrifuge where it is accelerated and transferred via the guiding system into the torus vessel [7].

In order to avoid too long ice rod storage times, the pellets were injected in consecutive trains of 10 large pellets. They were injected with a speed of 550 ms^{-1} at a rate of 15 Hz. A few pellets at the rod tip were discarded due to the variable composition in the onset of the extruded material.

After every pellet train, the residual gas was analysed with the QMS, which typically took several minutes to record the spectra. After several trains, the torus vessel was evacuated again in order to prevent a torus pressure rise into a regime regarded unsuitable for the analysis. The typical sequences as performed for the two Ar admixed rods are shown in Fig. 2. The evolution can be recognized by the sudden pressure rise caused by each arriving pellet train followed by the plateau phases where the QMS spectra were recorded. Hence, every measured spectrum refers to an average over 10, 20 or 30 pellets with the values of the second and third train to be obtained by deconvolution analysis. The runs processing the entire ice rods typically took 25–35 min; thus, the rear end of the rods had always been stored considerably longer than the front end.

For the considerations on the admixed pellet technique presented here, results from earlier works were also considered. This covers investigations of D_2 pellets with N_2 admixed [3] or mixtures of the two stable hydrogen isotopes H and D [2] in the AUG PLS, as well as using an ORNL extruder admixing up to 2 mol% Ne into D_2 [4,5]. Details of these experiments can be found in the according references. This study of noble gas admixtures in the AUG PLS was initiated by the EU-DEMO request to use Xe; details are published elsewhere [14]. An important result of the Xe experiment was that there is a potential issue with the amount and homogeneity of the admixed component in the ice rod prepared. Only a small fraction of the Xe provided in the gas sample was found in the ice and its distribution was patchy. Thus, although the same approach for the analysis was kept for the Ar and Kr admixtures, greater efforts were made to investigate this issue. The RGA analysis of an entire ice rod launched sequentially into the empty torus was performed twice for Ar in order to check its reproducibility. Together with one run performed with Kr and the already available Xe data set, results from 4 complete rods with 3 different gases are at hand.

A compilation of the RGA analysis results for all investigations of the

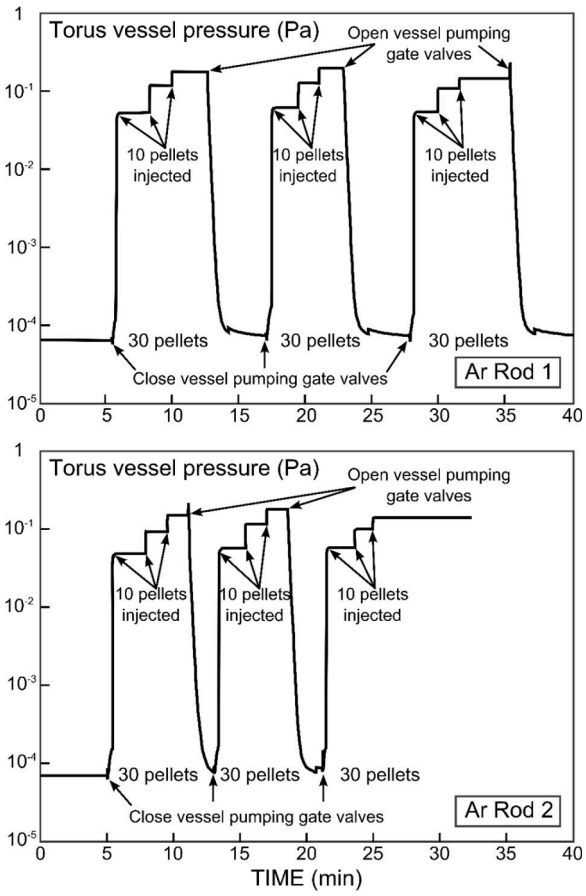

Fig. 2. Torus vessel pressure evolution recorded during the RGA analysis of two injected ice rods. Each arriving pellet train results in a sudden pressure rise; the following plateau phase indicates the QMS data acquisition time. To prevent a too high vessel pressure, the vessel was pumped after each third pellet train.

noble gas admixtures enlisted in Table 1 is displayed in Fig. 3. The data shown are taken from the previous Xe investigation where a single rod was applied [14], two separate runs with the Ar admixture and one with Kr in the ice. Clearly, there is a trend for a declining concentration along the ice rod but also a restricted reproducibility.

Evidently, it is possible to incorporate all stable noble gases in

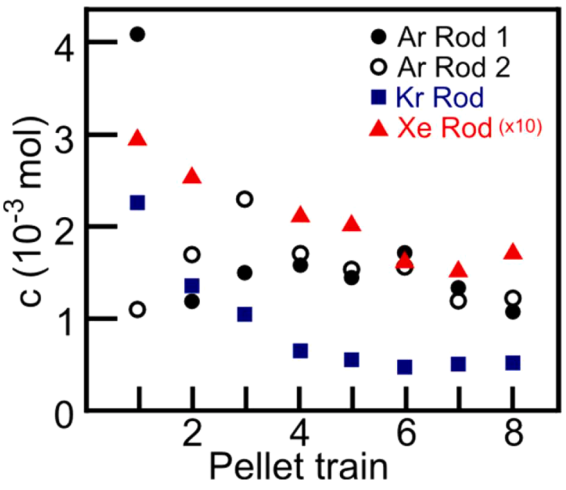

Fig. 3. Concentrations of noble gases found in the D_2 host gas released from smashed pellets in the torus. Each pellet train consisted of 10 large pellets injected at 550 ms^{-1}.

admixed pellets. However, the experiments with the AUG PLS showed limited reproducibility of the admixed concentration and a concentration which is always lower in the pellets then in the provided gas sample. Obviously, compared to the D_2 host gas, a smaller fraction of the admixed gas is sustained when parts of the provided sample gas get frosted in the extrusion cryostat. Taking the measured concentrations in the produced ice (c_{ice}) and in the supply gas (c_{gas}), the extend of this depletion effect occurring during the ice production can be quantified by the frosting ratio $\varepsilon_f \equiv c_{ice}/c_{gas}$. Notably, ε_f is specific for the employed pellet source configuration since the applied hardware configuration has a significant influence.

An overview of the ε_f values as calculated for the data available is plotted in Fig. 4. For the three noble gases investigated, averaged values are represented by black dots while the range of values found in different parts of the ice rods are indicated by the grey bars. Added are also the values from the initial investigation employing N_2 [3] and the hydrogen isotope mixture approach [2] performed with the AUG PLS and, considering the large ORNL extrusion performance as well [4,5], its already existing tests with Ne. As can be seen from Fig. 4, all the data get well ordered with respect to admix gas triple point temperature, indicating admixing into D_2 host pellets gets less efficient with this temperature increasing. As apparent from the insert of Fig. 4, it becomes generally also more intricate to admix gases with a higher Z. Also shown in the insert are the data of Oxygen (O_2) and Fluorine (F). Carbon (C) is also considerable as potential admixed substance in case methane (CH_4) respectively ethane (C_2H_6) is used.

4. Plasma actuation investigations

In addition to the RGA, for any admixed species at least one plasma discharge was performed dedicated to the admixed pellet actuator characterization; in addition, some experiments applying this tool took place. The analysis for the basic Xe/D_2 pellet impact on the plasma can be found in [14]. A real control application for the purpose of fast and efficient radiative power removal took place employing Ar, which is considered the most suitable choice for radiative power removal in AUG. A detailed analysis of these plasma experiments proving the beneficial properties of the pellet actuator but also its current technical limits can be found in [9].

As in the RGA experiments, the initial part of the ice rod was discarded as well in all plasma experiments. This is done to get rid of a potentially degraded or lost ice rod tip during the preparatory period for the plasma discharge.

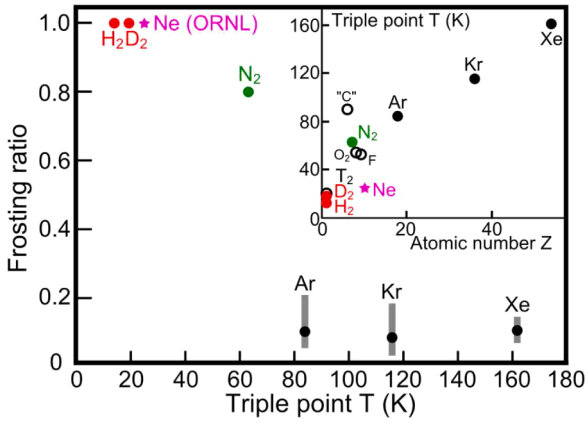

Fig. 4. Frosting ratio for different gas mixtures and extruder configurations used to produce admixed pellets. Data from this study (black dots: averaged; grey bars: range of values found) and previous referenced investigations versus triple point temperature. Insert: triple point temperature versus atomic Z number for several room temperature gases ("C" indicates methane CH_4 or ethane C_2H_6).

Presented for the first time in this study is the Kr radiator actuation via admixed pellets in a plasma discharge. A discharge where pellet actuation is compared to Kr gas puffing was conducted. The plasma was configured in the same quasi-continuous exhaust (QCE) high confinement mode that was previously used for the Ar seeding investigations [9], with a typical plasma shape as shown in Fig. 1. Important time traces are shown in Fig. 5. Until plasma termination was initiated at 6.8 s, steady auxiliary heating (7.3 MW neutral beam injection – NBI, and 3.6 MW ion electron cyclotron resonance heating –ICRH) and strong D gas puffing ($4\bullet10^{22}$ Ds^{-1}) was applied. From 2.96 to 5.07 s a pre-programmed train of small pellets was injected with a speed of 557 ms^{-1} at a repetition rate of 23 Hz; thus, the averaged pellet fuelling flux is about $3.5\bullet10^{21}$ Ds^{-1}. From the RGA Kr data a concentration of 0.2 mol % was taken as best estimate for the initial part of the pellet train around 3.5 s. This results in a flux of $3.5\bullet10^{18}$ Krs^{-1} as indicated by the solid line ("Pellet Kr flux estimation") in Fig. 5. The observed temporal evolution of the ablation radiation indicates pellets arrive in sound shape. Correspondingly, despite this moderate flux, the pellets cause a significant elevation of the plasma density. Like in the Ar case [9], no large edge localized modes (ELMs) are triggered by the pellets and the QCE conditions can be maintained. From 5.3 to 6.5 s, a gas mixture of D_2 hosting 22.7 mol% Kr is puffed; the flux magnitude was feedback controlled in order to set the power flux crossing the last closed flux surface (separatrix). In both seeding scenarios, the impact of the Kr on the plasma is clearly visible. The total radiated power from the plasma is significantly enhanced with respect to the applied auxiliary heating power. Hence, in turn the plasma energy is reduced. The impact of every single pellet can be clearly resolved even on these global plasma parameters, showing their fast actuation potential. A Kr monitor displays the local density calculated from the presence of Kr^{24+} (Mg isoelectronic sequence) as measured by the SPRED via the singlet transition $3s^2\ ^1S$ to $3s3p\ ^1P$ at 15.82 nm [15]. Clearly, the Kr amount carried per pellet decreases during the train while the pellet size is kept constant as can be concluded from the pellet monitor and overall plasma (electron) density n_e evolution. This indicates a decreasing Kr concentration in the supplied ice rod. Fuelling efficiencies of both seeding techniques can be compared when relating the estimated Kr flux of $3.5\bullet10^{18}$ s^{-1} during the pellet phase at 3.5 s to the $2\bullet10^{19}s^{-1}$ applied via gas puffing at 6.0 s. Since both effectuate a similar amount of Kr in the plasma, this confirms the advanced efficiency of admixed pellets.

5. Ar inventory in a plasma discharge with admixed pellet injection

As mentioned above, local Ar^{16+} densities can be derived from tailored CXRS measurements at AUG. For typical AUG plasma

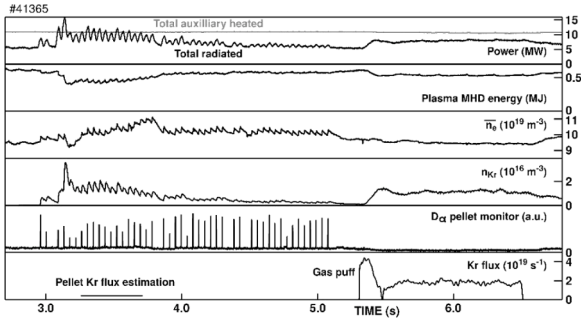

Fig. 5. Comparing Kr plasma delivery first via pellets and then by gas puffing. Plasma parameters like the total radiated power and the plasma energy clearly showing the impact of the Kr radiator. While the pellet size is obviously maintained during the train (as can be seen from the pellet monitor recoding the D_α ablation radiation and the density evolution) the Kr flux is not. Yet, during the first part of the train pellets unveil a faster and more efficient Kr delivery than the gas puff.

parameters, the He-like charge state Ar^{16+} is of most interest, as it typically exists over the widest range of the plasma. Thus, the total Ar density can be estimated from the Ar^{16+} data, typically assuming $n_{Ar} = 1.2\ n_{Ar^{16+}}$, with $n_{Ar^{16+}}$ taken at its maximum value in the radial profile. In this study, CXRS measurements of Ar^{16+} were taken during an experiment performed for commissioning and testing of the PLS operated with Ar admixed pellets. The acquired data were used to analyse the amount of admixed matter delivered with the pellets. In the experiment, a train of large pellets with 550 ms^{-1} was launched into a routinely run robust 1MA "standard H-mode" discharge. The repetition rate and hence the flux were increased stepwise: 23 Hz from 4.0 to 5.0 s, 35 Hz from 5.0 – 5.5 s, and 70 Hz from 5.5 to 6.5 s, reaching the maximum available pellet flux of $2.6\bullet10^{22}$e s^{-1}. Throughout, D_2 gas was puffed at a rate of $2.0\bullet10^{22}$e s^{-1}.

The time traces of relevant parameters are displayed in Fig. 6; boxes from top to bottom: the total radiated power (black) and total applied auxiliary heating power (grey, NBI and ICRH); the "validated" line averaged density calculated from Bremsstrahlung calibrated with respect to the core DCN measurement [16]; the total plasma electron particle inventory N_e of the confined plasma region as calculated by an integrated data analysis of all the available valid profile diagnostics [17]; the line radiation of three different Ar ionization stages measured by the SPREAD spectrometer; the total Ar atom inventory N_{Ar} of the confined plasma region estimated from the CXRS measurements of Ar^{16+}; the pellet monitor. For comparison, in the box with the N_{Ar}, data the estimated maximum amount of Ar atoms enclosed in a single pellet of $3.7\bullet10^{17}$ is indicated. This is based, as for the Kr case, on the assumption of a maximum concentration of 0.2 mol% Ar in the ice. Thus, it is estimated the maximum available pellet flux of $2.6\bullet10^{22}$e s^{-1} can carry an Ar flux of about $2.6\bullet10^{19}$Ar s^{-1}.

As in the previously discussed plasma experiments, a decreasing concentration of Ar in the admixed pellets is observed. Considering the phase around 4.7 s, where the highest Ar amount per pellet is still present, the observed pellet induced rise of N_{Ar} matches well with the assumption on the maximum Ar content in a single pellet. As apparent from the radiation time traces the Ar content in the plasma is still strongly modulated while the lowest pellet rate is applied; a steadier behaviour is reached when the injection rate is increased. Thus, it can be concluded that the Ar confinement time is around the initial pellet repetition time of about 40 ms. During the initial phase, N_e is raised to about $11\bullet10^{20}$ from an initial value of about $9\bullet10^{20}$ by a pellet flux of $8.5\bullet10^{21}s^{-1}$. Taking this fuelling impact as guideline, the overall pellet particle sustainment time can be estimated as $\tau_P^* = 2\bullet10^{20}/8.5\bullet10^{21}s^{-1} \approx 24$ ms. This overall sustainment time and the assumed Ar flux of $8.5\bullet10^{18}$ s^{-1} in the initial phase, calculated from the maximum Ar content in a pellet, would yield an expected averaged Ar content level of about $2\bullet10^{18}$. This is in reasonable agreement with the estimated N_{Ar} values. 23 Hz are still too low in order to create a steady Ar level, switching to higher rates effectuates a smoother evolution yet at a declining level due to the fading concentration in the pellets. While the step to 70 Hz rate first increases the Ar level again, the supposedly further dwindling concentration leads to the roll over towards in the final part.

The same sequencing is observed in the temporal evolution of the Ar^{16+} density profile reconstructed from CXRS data as shown in Fig. 7. The highest peak with a density of about $7\bullet10^{16}$ m^{-3} is found at about 4.76 s at a major radius of R = 1.95 m. There, the plasma electron temperature is about 1 keV and the electron density about $1\bullet10^{20}$ m^{-3}. Approximating the D density by the electron density, the local concentration of Ar^{16+} ions in the plasma is estimated about $7\bullet10^{-4}$. This is a remarkable result, since it comes close to the estimated maximum atomic Ar concentration of $1\bullet10^{-3}$ in the pellet itself. With pellets arriving from the torus inboard while the CXRS observes the plasma outboard, their locations can be mapped referring to the poloidal magnetic flux surfaces ρ_{pol}. The Ar^{16+} peak is found at about $\rho_{pol} = 0.6$. Ablation of the according pellet lasts 0.64 ms, thus a flight at the initial speed along the designated (tilted) trajectory yields a penetration depth of 0.35 cm, i.e. reaching up to about $\rho_{pol} = 0.7$. Apparently, the pellet had arrived in sound shape and the ablated pellet material gets shifted a bit further inward by the plasmoid drift effect in tokamaks [18]. The fading concentration in the ice is well reproduced by the Ar^{16+} ion presence; which is transitory compensated by the higher flux after 5.6 s. In this final phase, the stronger pellet fuelling results in higher core plasma densities and a cooler plasma allowing for deeper pellet penetration and deposition; accordingly, the Ar^{16+} peaks are shifted inwards, too. Little Ar is transported towards the plasma centre in the first and second phase but Ar appears at least transiently in the plasma centre at $R = 1.71$ m in last phase. However, this is during a phase where the very strong pellet fuelling creates a peaked density profile and the pellets penetrate deeper. Apparently, the desired local deposition of admixed matter can be achieved and, in case core accumulation is avoided, also its fast removal. A smooth evolution can be reached if reasonably sized pellets with a homogeneous admixture of the designated component at an appropriate concentration are injected at a sufficiently high rate.

6. Discussion

As repeatedly proven, a variety of admixed pellet types can be produced and applied as advanced actuators for plasma control issues. In particular, the supply of the admixed components is more efficient and faster than achieved by simple gas puffing. Our recent investigations focusing on noble gases cover experiments in which admixed pellets were injected into plasma discharges for actuator commissioning and characterization as well as for first actuator applications. In addition, the pellet composition was carefully analysed by RGA of the released gas after the injection of pellets into the AUG vessel without plasma. Good qualitative and reasonable quantitative agreement was found for the

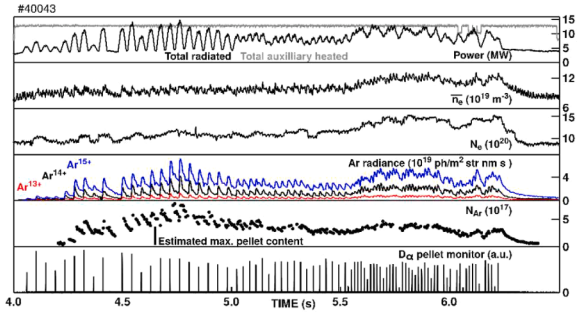

Fig. 6. Train of pellets with admixed Ar injected in a robust "standard" plasma configuration; repetition increasing in 3 steps to the technically possible maximum. The total Ar content inside the confined plasma N_{Ar} is estimated from CXRS measurements of the Ar^{16+} ion density. Indicated is as well the estimated maximum Ar content in a single pellet.

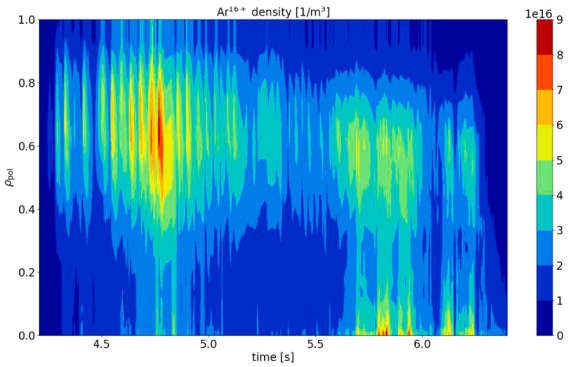

Fig. 7. Spatiotemporal evolution of the Ar^{16+} ion density as measured with CRXS.

results from the RGA and the behaviour observed during plasma operation and the detailed investigation of the total Ar content in the confined plasma based on CXRS measurements. The admixed species is significantly depleted in the ice with respect to the used gas sample; this effect is more pronounced with increasing triple point temperature. In addition, the admixed concentration distributions within the ice rods are scattered. This can be attributed to the ice-production setup of the AUG PLS, which is not laid out for this task. In particular, the extrusion cryostat is cooled to the D_2 freezing temperature in order to solidify the incoming supply gas; but no option is yet available to keep the adjacent gas supply line above freezing temperature of the admixed gas. Hence, likely a considerable amount gets condensed already in the supply line. This effect is acting as a cryo-distillation, having an influence on the final concentration of the admixed species in the extrusion cylinder. As an additional consequence, the supply line got blocked after one or two extrusion runs and had to be warmed up. Lacking a dedicated RGA equipment in the launcher setup no detailed analysis of the gas release during the warming up could be made. However, during recovery the most significant gas release only took place well beyond the triple point temperature of the according admixed gas.

Self-evidently, more sophisticated and adapted system are required for the handling of admixed gases. For example, the large volume ORNL extruder has been found capable to handle Ne well. Yet, the extrusion speed is slowed down and the achievable mass throughput is reduced accordingly. In summary, the presented initial explorative investigations clearly reveal the great potential of the admixed pellet actuator tool, although they also demonstrate that further technology efforts are required before their benefits can be fully utilized.

7. Outlook

In our setup the solid is condensed directly from the admixed gas phase at a temperature solely optimised for freezing the D_2 host. This approach purely relies on the admixed species' frosting respectively co-deposition in the ambient ice host and is constrained to a small concentration level of the added substance. However, this rather unsophisticated and simple approach works turned out capable to produce ice at a quality adequate for the formation of stable pellets. As proven by the flawless delivery of large pellets at an elevated speed the available admixed pellets unveiled the same permissive load during acceleration and transfer as their pure D_2 counterparts. Apparently, the presence of an admixed component in the realised concentration range keeps the mechanical pellet properties undiminished. It is this stability resilience keeping the pellets suitable for the initial proof-of-principle investigations and the first follow-up applications as reported – admittedly with the caveats as described.

As a next step to improve the situation, it is envisaged to implement an additional temperature control of the supply line in order to prevent cryo-distillation of the admixed gas and thus at least mitigate the observed depletion effect. Though, in view of EU-DEMO, concepts are required capable to handle either much larger quantities in a batch process or even steady state extrusion as e.g. in a screw extruder [19]. This implies a technological challenge. While hydrogen mixtures composed from any of the six different isotopologues H_2, HD, HT, D_2, DT and T_2 are miscible in all phases at least down to 4 K, little is known yet about the miscibility of the hydrogens with other substances [20]. Ne is considered to be the noble gas that is easiest to handling since its triple point temperature is closest to that of the hydrogens. And, following helium, Ne is the most studied element in mixtures with hydrogen. For example, a temperature-composition diagram exists for D_2—Ne showing a common liquid phase at the D_2 side with the adjacent eutectic point at 18.5 K for 2.3 mol% dissolved liquid Ne [20]. Tests with the ORNL extruder [4,5] unveiled that the ice with the admixed species likely simply mechanically entrained is sufficiently adhesive allowing for its extrusion into long stable and lasting rods. While Ne admixing could thus work up to a certain extent directly from the initial supply gas with an interstage attemperator liquefier stage, most other gases and especially – due to their much higher triple point temperatures – the other noble gases will likely need a different approach. For example, it could be considered to form noble gas layers on the hydrogen ice – or vice versa, since for Ar, Kr and Xe porous layers formed at temperatures below approximately 0.25 of the corresponding triple point temperature exhibit a high sorption capacity for hydrogen, allowing them to store large quantities, and act, in effect, as a pump [21].

Declaration of Competing Interest

The authors declare that they have no known competing financial interests or personal relationships that could have appeared to influence the work reported in this paper.

Data availability

Data will be made available on request.

Acknowledgements

This work has been carried out within the framework of the EUROfusion Consortium, funded by the European Union via the Euratom Research and Training Programme (Grant Agreement No 101052200 — EUROfusion). Views and opinions expressed are however those of the author(s) only and do not necessarily reflect those of the European Union or the European Commission. Neither the European Union nor the European Commission can be held responsible for them.

References

[1] C. Day, et al., Fusion Eng. Des. 179 (2022), 113139.
[2] P.T. Lang, et al., Nucl. Fusion 59 (2019), 026003.
[3] B. Ploeckl, et al., Fusion Eng. Des. 96-97 (2015) 155.
[4] P.T. Lang, et al., Fusion Eng. Des. 166 (2021), 112273.
[5] L.R. Baylor, et al., Fusion Sci. Tech. 77 (2021) 728.
[6] M. Siccino, et al., Fusion Eng. Des. 176 (2022), 113047.
[7] B. Ploeckl, et al., Rev. Sci. Instrum. 84 (2013), 103509.
[8] V. Rohde, M. Oberkofler, ASDEX upgrade team, J. Nucl. Mater. 463 (2015) 672.
[9] A. Kallenbach, et al., Nucl. Fusion 62 (2022), 106013.
[10] IUPAC, Compendium of Chemical Terminology, 2nd ed., the "Gold Book, 1997 https://doi.org/10.1351/goldbook.T06502.
[11] J.R. Rumble, ed., CRC Handbook of Chemistry and Physics, 103rd ed. (Internet Version 2022), CRC Press/Taylor & Francis, Boca Raton, FL.
[12] R.M. McDermott, et al., Plasma Phys. Control. Fusion 60 (2018), 095007.
[13] R.M. McDermott, et al., Nucl. Fusion 61 (2021), 016019.
[14] P.T. Lang, et al., Fusion Sci. Tech. 77 (2021) 42.
[15] E.B. Saloman, J. Phys. Chem. Ref. Data 36 (2007) 215.
[16] P.T. Lang, et al., Nucl. Fusion 58 (2018), 036001.
[17] R. Fischer, et al., Fusion Sci. Tech. 58 (2010) 675.
[18] P.B. Parks, L.R. Baylor, Phys. Rev. Lett. 94 (2005), 125002.
[19] S.J. Meitner, et al., Fusion Sci. Tech. 56 (2009) 52.
[20] P.C. Sours, Hydrogen Properties for Fusion Energy, University of California Press, 1986.
[21] H. Abe, W. Schulze, Chem. Phys. 41 (1979) 257.